International Journal of
Nanoscience and Nanotechnology

Research Article 2025, Volume 21, Issue 2

Uncovering the properties of nanoemulsion loaded with *Boswellia serrata* essential oil: Synthesis, characterization, stability, and in vitro biological activity

Arun Dev Sharma[1*], Amrita Chauhan[1], Inderjeet Kaur[1], Ravindresh Chhabra[2], Puneet Jain[2], Ranjna Devi[2]

Received 5 February 2025
Accepted 20 May 2025

DOI: 10.22034/ijnn.2026.2052707.2630

International Journal of Nanoscience and Nanotechnology

Abstract

Guggul essential oil (GEO) derived from Boswellia serrata is utilized in ayurveda as traditional and complementary medicine. However, because of its chemical instability, volatile nature, strong aromas, and poor absorption, the use of GEO is restricted. The objectives of this work were to create GEO-oil-based O/W (oil/water) nanoemulsions (GNE) and evaluate its biological potential. GNE were prepared by using Tween-80, ethanol and SDS with an ultrasonicator. Physicochemical characterization was completed using a particle size analyzer, UV, fluorescence, and FT-IR methods. Numerous biological activities, such as anti-inflammatory, antidiabetic, antibacterial, and anticancer were estimated. The spherical-shaped nanoemulsions had globule size of 220 nm, zeta potential of -35.30 mV, polydispersity index of 0.25, and drug entrapment efficiency of 96.5% (w/v). GNE's in vitro drug release occurred slowly roughly 45% at six hours. GNE exhibited remarkable antioxidant potential such as: 72% for scavenging DPPH radicals, 40% for scavenging ABTS radicals, 28% for scavenging hydroxyl radicals, and 81% for the iron chelating. Antibacterial activity was observed with inhibition zones ranging from 0.3 to 1.1 cm against Gram-positive and Gram-negative bacteria. After being exposed to 5 µL of GNE, 20% of HeLa cells were viable. GNE exhibited 70% inhibition of α-amylase activity at its higher dose of 250µL. GNE remained stable even for 50 days. Drug release kinetics showed that GNE followed the Higuchi model. GNE's potential in the pharmaceutical and food industries has also been explored.

Keywords: Essential Oil, Biological Activities, Nanoemulsion, Tween-80, Boswellia Serrata, Guggul

How to cite this article
Sharma AD, Chauhan A, Kaur I, Chhabra R, Jain P, Devi R. Uncovering the properties of nanoemulsion loaded with Boswellia serrata essential oil: synthesis, characterization, stability, and in vitro biological activity. Int. J. Nanosci. Nanotechnol., 2025;2: 97-107. DOI: 10.22034/ijnn.2026.2052707.2630

1. Introduction

Essential oils are used in cosmetics, fragrances, makeup, and natural remedies, along with antimicrobial agents as food additives and preservatives [1,2].

The medium-sized, branching tree *Boswellia serrata* is an ancient and highly valued plant in ayurveda, and it is a member of the Burseraceae family [3]. The Burseraceae family, which comprises approximately 17 genera and 600 species, is distributed throughout tropical regions worldwide. The genus *Boswellia* has about twenty-five species, most of which are found in the Arabian Peninsula, Ethiopia, Somalia, India, and the northeastern coast of Africa [4]. *Boswellia serrata* exudes an oleo-gum resin also known as *Salai* or Guggul [5]. It is a resin whose aromatic smoke is traditionally used to relieve laryngitis, bronchitis, asthma, and other respiratory ailments. Because of its remarkable antibacterial and antifungal properties, *Boswellia serrata* essential oil is appropriate for use in food preservation [6]. Certain studies suggest that GEO can protect grains from fungal growth by reducing the levels of harmful aflatoxins released by Aspergillus species. Furthermore, GEO exhibits potent antibacterial activity against a variety of pathogens responsible for food spoilage [6,7]. Hydro-distilled GEO has long been utilized in ayurvedic and traditional chinese medicine for a range of ailments, including arthritic and inflammatory ones [8]. Numerous ailments, including cancer, psoriasis, arthritis, and asthma, have been treated with it [6]. It has been utilized in traditional medicine for its antiseptic, antiarthritic, and anti-inflammatory properties since ancient times [6]. A number of bioactive substances were discovered in the GEO, including major and minor constituents such as caryophyllene

[1] *Department of Biotechnology, Lyallpur Khalsa College, Mohyal Nagar Jalandhar, Punjab (144008), India*

[2] *Department of Biochemistry, Central University of Punjab, VPO Ghudda-151401 Bathinda. India*

E-mail: arundevsharma47@gmail.com

alcohol, limonene, thujene, pinene, octanol, and linalool [9,10]. However, because of its unstable nature, limited water solubility, and light sensitivity, GEO is not widely used in the food and pharmaceutical sectors [11]. Essential oils are readily degraded by heat, light, air, and moisture. Therefore, proper methods are necessary to address these limitations, which may lead to the loss of pharmacological and qualitative attributes [11]. Therefore, the process known as encapsulation shields essential oils from the external environment to maximize the stability and bioavailability of these molecules [12-14]. In this respect, the field of nanotechnology has great promise, particularly for the development of nanoemulsions. Nanoemulsions are aqueous systems containing small internal-phase oil droplets with size ranging from 20 to 1000 nm therefore improving the dispersion of hydrophobic constituents. Strong kinetic stability protects nanoemulsions from creaming, sedimentation, and phase separation [15]. The two primary types of nanoemulsions (NE's) are oil-in-water (O/W) and water-in-oil (W/O). Bioactive compounds present in nanoemulsion droplets are protected from air, light, and other unfavourable environmental factors [15]. As mentioned earlier, the use of GEO in different sectors is restricted by several physicochemical limitations, thus necessitating encapsulation-based approaches to promote the wider use of essential oils derived from *Boswellia serrata* in the food, pharmaceutical, and cosmetic industries [16-18]. In the previous study, the phytochemical profile of GEO was reported and its diverse biological activities were evaluated [19]. In the continuation, the objective of this study was to formulate nanoemulsions based on *Boswellia serrata* essential oil and evaluate its biological activities, including antidiabetic, antibacterial, antioxidant, anticancer, and anti-inflammatory, along with its *in vitro* release profile**.**

2. Material and Methods

2.1. Extraction of essential oil

Guggul essential oil (GEO) was used for this investigation. The oil was extracted by hydro-distillation of *Boswellia serrata* oleo gum-resin, which was kindly supplied by Wommune, Bioryca Healthcare Pvt Ltd. With minor modifications, standard colorimetric techniques were used to estimate the total phenolic, total flavonoid, and total tannin content of GEO following the description provided in [20].

2.2. Preparation of GNE (ultrasonication method)

In 85 mL of water (double-distilled), 5% Tween-80 (v/v), 5% ethanol (v/v), and 0.25% sodium dodecyl sulphate (SDS) (w/v) were added at room temperature (~30 °C). The mixture was then heated to 50 °C and allowed to become translucent. The resultant mixture was vigorously agitated for 15 minutes at 2000 rpm using a magnetic stirring device (Model 2MLH, Remi Ltd., India), and then 5% (v/v) GEO was added drop-wise. After agitating the crude nanoemulsion (GNE) mixture for 20 minutes, an ultrasonicator bath (Citizen CDT, UC-2000) with an ultra-high frequency was used to sonicate it for 1 hour at 20 °C and 25 kHz. After that, the nanoemulsions (GNEs) were stored at 4 °C.

2.3. Fingerprinting analysis and characterization

Fluorescence, UV–Vis, and FT-IR spectroscopy were used to characterize the generated GNE as briefed previously [20]. Physicochemical properties, including conductivity, pH, turbidity, dilution test, % transmittance, and the dye solubility were evaluated using newly synthesized GNE [20]. Utilizing the MicroView microscope equipment (Debro DM RL), the GNE were observed following the instructions described previously [20].

2.4. Stability studies of GNE

The GNE formulation's stability was evaluated [20]. For this, 5 mL of GNE was placed inside sealed glass vials. These vials were kept at a constant temperature (RT: 37 °C ± 8), -20 °C, and 4 °C for 50 days. Visual evaluations were conducted on GNE samples to determine their phase separation, drug precipitation, and transparency. The GNE formulations were also subjected to centrifugal tests for stability. After spinning for 30 minutes at 6000 rpm (Remi, India centrifuge machine), the GNE samples were inspected for drug accumulation, phase separation, and transparency.

2.5. Determination of particle size

The particle size and zeta potential of GNE were determined using a Particle Size Detector (Malvern Zetasizer Nano ZS90, UK) and Zetasizer Nano ZS (Malvern Instruments) as per manufacturer instructions.

2.6. HR-TEM analysis

To get structural insights of GNE, high resolution-transmission electron microscopy (HR-TEM) was employed as the method described earlier [21]. The GNE were diluted with distilled water as per manufacturer instructions. Then, for 60 seconds, the samples were adsorbed onto 300 mesh grids of copper covered with carbon. The grids were then inspected utilizing HR-TEM analysis (JEM-2100 Plus, JEOL, Tokyo, Japan) for morphological observation.

2.7. Drug entrapment efficiency (DEE) and drug release (DR)

As described earlier [21], DEE and DR analysis were conducted using a UV–Vis spectrophotometer (Labtronics, India) calibrated at 210 nm. The drug release profile of GNE was analyzed by looking at the Higuchi model, Korsmeyer-Peppas model, first-order kinetic, and zero-order models.

2.8. Antioxidant activity analysis

Many antioxidant tests like DPPH (2,2-diphenyl-1-picrylhydrazyl), ABTS (2,2'-azino-bis-(3-ethylbenzothiazoline-6-sulfonic acid)) radical scavenging activity, hydroxyl radical scavenging activity, iron reducing assay, and iron chelating assay were used to evaluate the antioxidant ability of GNE following Sharma et al. [20].

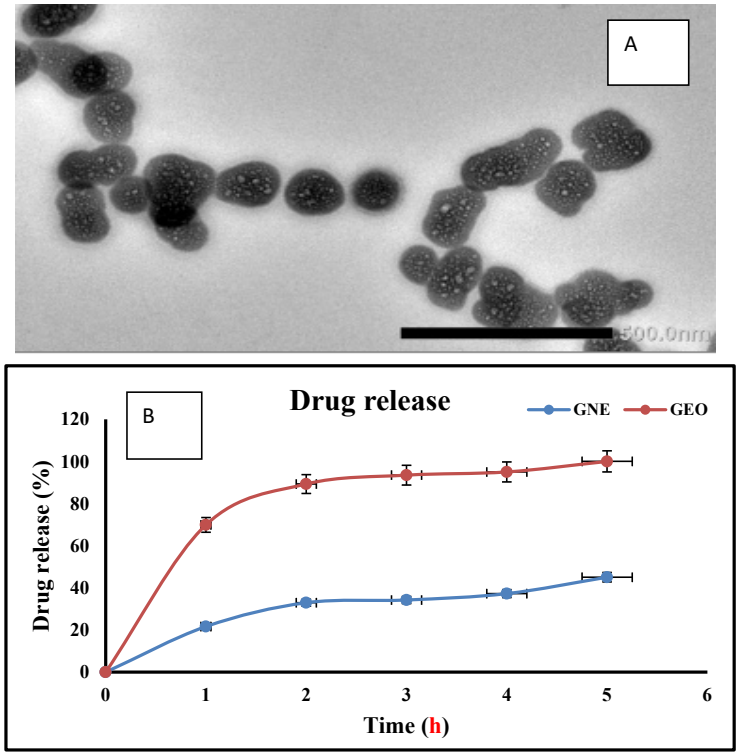

Figure 1. Characterization and release profiles of GNE. (A) Representative HR-TEM image showing the spherical morphology of the GNE formulation (scale bar: 500 nm). (B) *In vitro* release profile of GNE compared with pure GEO.

2.9. Anti-inflammatory activity (protein denaturation) of GNE formulation

A fluorescence assay was employed to evaluate the protein denaturation assay [21]. The reaction mixture contained 1% w/v BSA (400 µL), 1 × PBS (pH 6.4; 4.78 mL), and 100–300 µL of GNE. After incubating at 37 °C in a water bath for 15 minutes, the resultant mixture was heated at 70 °C for 5 minu

tes. The reaction mixture was immediately cooled. One mL of reaction mixture was put into quartz cuvettes for fluorescence measurement (fluorescence spectrophotometer from Perkin Elmer, FL6500). The emission spectrum comprised 300 to 400 nm, and 280 nm was the excitation wavelength. Paracetamol and Combiflam, standard drugs, were used as positive controls (10 µg/mL).

2.10. Anti-α-amylase activity of GNE

Anti-amylase potential of GNE was evaluated following Chauhan et al. [21]. The standard or positive control was acarbose (1 mg/mL). A reciprocal plot of 1/[S] vs 1/[V] was plotted. Through the use of Michaelis-Menten kinetics and Lineweaver-Burk plot, the mechanism by which GNE inhibits α-amylase activity was determined.

2.11. In vitro antibacterial activity of GNE formulation

The antibacterial activity of GNE was assessed using the agar disc diffusion method following Chauhan et al. [21] against four test species: Gram-positive *Staphylococcus aureus* (MTCC 3160), Gram-negative *Escherichia coli* (MTCC 40), Gram-positive *Bacillus subtilis* (MTCC 121), and Gram-negative *Pseudomonas aeruginosa* (MTCC 424). The zone of inhibition (ZOI), the radius surrounding the disc, was measured and recorded, demonstrating the antibacterial activity of GNE. The cytoplasmic content released (CCR) denotes the amount of UV-absorbing material that seeped out of the bacterial cells.

2.12. Cytotoxicity assay of GNE formulation

Cytotoxicity effect of GNE was observed on HeLa cells, as described previously [21]. Briefly, the NCCS, Pune, India provided the HeLa cells, which were then grown in RPMI medium supplemented with 10% w/v Fetal Bovine Serum (FBS) and 1% v/v penicillin-streptomycin solution under standard conditions (5% CO_2 and 95% humidity at 37 ºC). Twelve hours before treatment, a 96-well plate containing about 10,000 cells per well was prepared for the cytotoxicity experiment. Three different concentrations of GNE (1 µL, 2 µL, and 5 µL) were applied to the cells. A positive control of paclitaxel (2 nM, 5 nM, and 10 nM) was employed. The cells were washed with 1 × PBS, after which MTT (5 mg/mL) was applied to each well. Then, in a CO_2 incubator, the plate was incubated for 4 hours. After dissolving the purple formazan crystals in 200 µL DMSO, the absorbance at 570 nm was measured using a microplate reader.

2.13. Statistical analysis

The Post Hoc Tukey HSD (beta) test was performed using SigmaStat (version 4.0) to determine $p < 0.05$. All values are expressed as mean ± SD (n = 3).

3. Results and Discussion

3.1. Physicochemical properties of GNE formulation

Morphological analyses revealed that the GNE produced were smooth, spherical, and non-aggregated

Table 1. physicochemical properties of essential-oil-based GNE formulation from Boswellia serrata.

physicochemical properties	Values
Type	o/w
pH	7.7 ± 0.5
Conductivity	0.431 ± 0.03 mS/cm
Zeta Potential (ζ)	-35.30 ± 0.23 mV
Mean Diameter	210.2 ± 10 nm
Polydispersity index (PDI)	0.25 ± 0.06
Turbidity	0.270 ± 0.08
% Transmittance	85.6 ± 0.4%
Drug entrapment efficiency (DEE) (w/v)	96.5 ± 8%

o/w: oil/water, PDI: polydispersity index. Values are mean ± SD (n=5).

(Figure 1A). GNE were kinetically stable. The entrapment efficiency of GNE was 96%, indicating that GNE have a significant capability for entrapping drugs [15]. Figure 1B displays the percentage release. It was discovered that, at 6 hours, the *in vitro* drug release of pure GEO was around 100%, but that of GNE was just 45%. As per the research published earlier [22], nanoemulsions have surfaced as a novel drug delivery technique that facilitates the controlled and extended release of a drug or biological active ingredient. The mean diameter of the synthesized GNE in the current investigation was 210 nm, and PDI was 0.25 (Table 1). Determining the nanoemulsions' particle diameter is therefore crucial [23]. These values suggested that GNE were of excellent quality. A measurement of droplet size homogeneity in nanoemulsions is called PDI. The overall stability and homogeneity of the GNE were shown by its low polydispersity index (PDI). Moradi et al. (2019) [24] discovered comparable PDI values, which supported the findings. The PDI of a formulation is a crucial factor in determining its stability. The PDI can range from 0 to 1, with 1 denoting a polydisperse system and 0 denoting a monodisperse system, according to Baboota et al. (2007) [25]. Low PDI values, according to Jaiswal et al. (2015) [17], frequently indicate constancy in the droplet size of nanoemulsions, which explains why globules typically hold together during long storage times. According to Table 1, the zeta potential value of GNE was -35.30 mV, indicating that the nanoemulsions were electrostatically stabilized [26]. Zeta potential (ZP) values are indicative of the innate forces that exist between the particles at the nanoemulsion surfaces, contributing to the stability of the material at an apparent scale [27]. For nano-formulations to be kinetically stable, ZP needs to be within ± 30 mV [27]. Table 1 shows that the pH of the GNE was 7.7 ± 0.5, which was steady. Electrical conductivity is represented by conductivity. Table 1 indicates that GNE's conductivity was 0.431 mS/cm. Farooq et al. (2021) [28] observed similar findings while they were creating miconazole nanoemulsions to treat *Candidiasis albicans*.

3.2. Fingerprint analysis of GNE formulation

Sharp peaks with an absorption of 3.0 at 240-340 nm were seen in the UV–Vis spectrum for GEO (Fig. 2A), suggesting the occurrence of secondary metabolic products such as tannins, flavonoids, and phenol compounds [21, 29]. Notably, GNE showed higher absorbance after GEO was encapsulated compared to GEO's pure UV–Vis spectra, suggesting GEO's successful encapsulation in GNE. It might be explained by the smaller particle sizes of high surface-area nanoemulsions. Laxmi et al. (2015) [27] observed a similar phenomenon after encasing artemether O/W nanoemulsions. The Green Fluorescent Region (GFR) has a prominent peak at 450 nm (main) and 500 nm (minor). It has been proposed that the biologically active substances in the GFR (450–500 nm) zone include polyphenolic compounds, including terpenoids, flavonoids, and flavins [29,30]. Significantly, a convincing rise in fluorescence intensity was seen at 500 nm from 1.2×10^5 to 1.9×10^5 when GEO was entrapped in the form of nano-formulations (Fig. 2B). The small surface area of the nanoemulsion globules, which provided a large interfacial area, may be responsible for this increase in the fluorescence signal. This outcome was consistent with the findings of the Laxmi et al. (2015) [27], which mentioned improved absorption during the creation of artemether O/W nanoemulsions. In another study, it was demonstrated that microemulsion enhanced fluorescence signals [31]. The authors claimed that since nanodroplets act as optical signal amplifiers, hence enhancing light scattering. By using FT-IR spectroscopy, the GEO entrapment inside its nanoemulsion form was assessed further. It was also evident that there was emergence of peaks when GEO was encapsulated (Fig. 2C). For example, two strong bands were identified in GNE at 3299 and 1639 cm^{-1}, which were not present in pure GEO. Upon encapsulation, a few significant and small peaks in the pure GEO IR spectra vanished. The formation of new bands demonstrated that, throughout the process of creating GEO nanoemulsion droplets, GEO effectively contained the mixed surfactant micelle structure. Yan et al. (2019) [16] observed similar alterations in FT-IR peaks and the appearance of new peaks when encasing bifenthrin, a biodiesel, in O/W-type nanoemulsions.

3.3. Storage effect on physicochemical properties of GNE

There were no signs of phase change, emulsification, or cracking during centrifugation. Since there was no gravitational separation, the kinetic stability of the GNE nanoemulsion was maintained. Emulsion stability is the most crucial element of nanoemulsion production in drug delivery systems, as it fluctuates with the pH level, temperature, storage duration, processing method, and ionic strength [26]. Furthermore, after 50 days of storage at different temperatures (4 °C, -20 °C, and RT), GNE were assessed in this work for longevity and shelf-life resilience (data not shown). Although microscopic

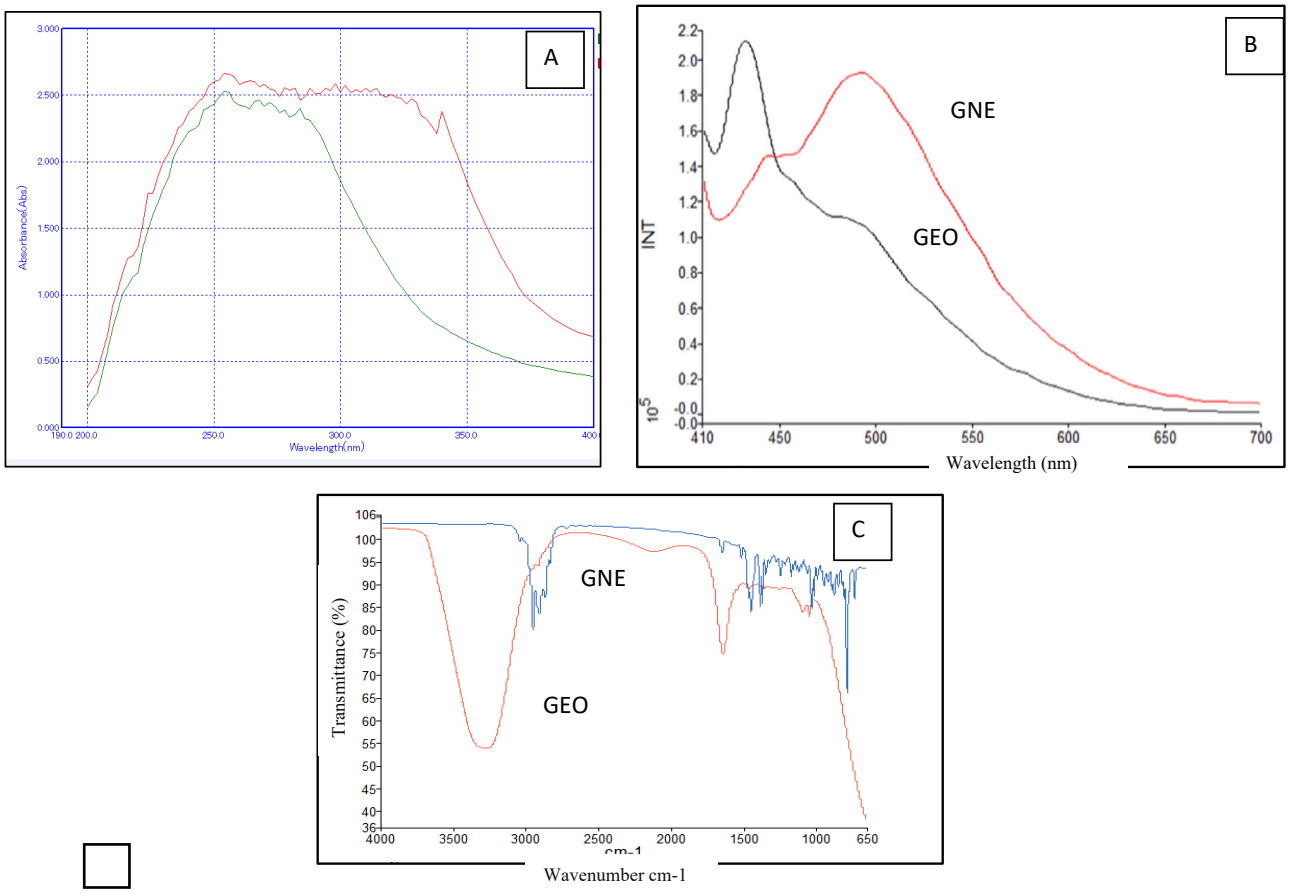

Figure 2. UV–Vis spectra (A), Fluorescence spectra (B), FT-IR spectra (C) of formulated nanoemulsions. GNE: nanoemulsion formulation; GEO: pure oil. INT: intensity

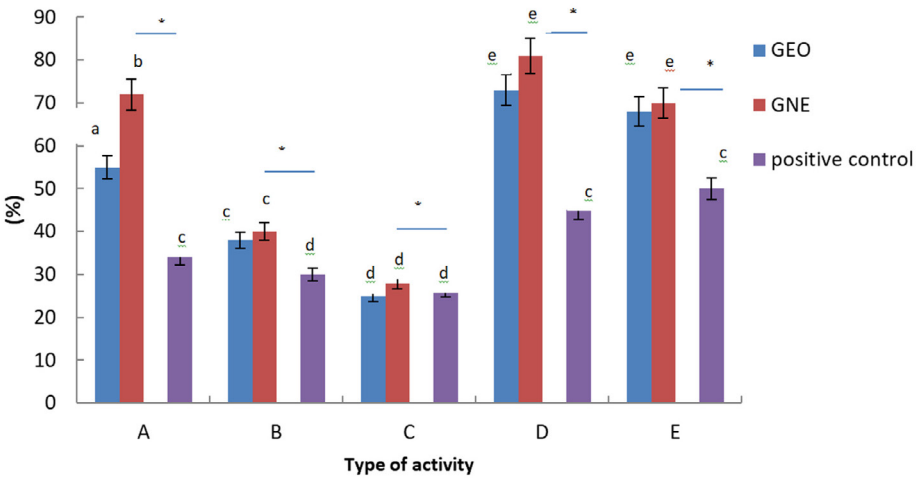

Figure 3. *Different biological activities depicted by pure oil (GEO) and nanoemulsions (GNE). (A) DPPH radical scavenging activity, (B) ABTS radical scavenging activity, (C) Hydroxyl radical scavenging activity, (D) Iron chelating activity, and (E) Alpha-amylase inhibition. Values are mean (n* **= 3) ± SD. The means followed by same letter at top of the bar are not significantly different at P < 0.05.** ** indicates significant difference of GNE vs positive control at P < 0.05*

examination of GNE at room temperature demonstrated flocculation, creaming, coalescence/Ostwald ripening, and phase separation, the particle size of GNE remained stable at 4 °C and -20 °C.

These findings support previous findings indicating that NEs are frequently vulnerable to creaming due to Ostwald ripening [29, 31]. Thus, it was essential to prevent Ostwald ripening during cold storage. It shows that because GNE were stable for 50 days at 4 °C and -20 °C, they could be the best options for industrial applications.

3.4. *In vitro* antioxidant analysis of GNE formulation

Figure 3 illustrates the diverse antioxidant potential of GNE. For instance, the activity of DPPH in scavenging radicals was 72%. Likewise, GNE demonstrated 40% ABTS scavenging activity. The evaluation of hydroxyl radical

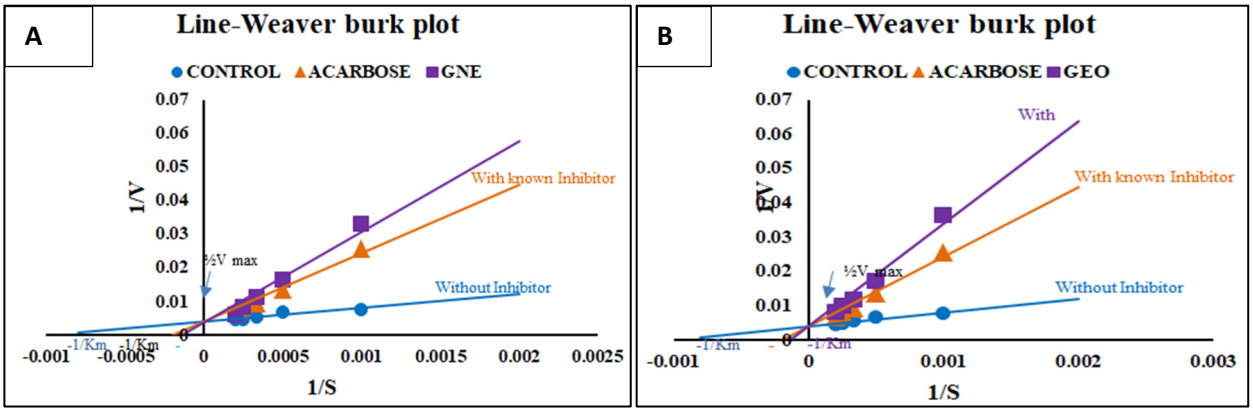

Figure 4. Lineweaver-Burk plot of GNE (A), GEO (B).

scavenging activity revealed 28%. The metal-chelating potential of GNE was 81%. The statistical analysis executed displayed the existence of a highly significant difference between the values of the reference compounds (ascorbic acid/ EDTA) and GNE $p < 0.05$. For example, positive controls exhibited 34% DPPH scavenging, 30% ABTS scavenging, and 45% metal chelating activities. Further, a comparative study of pure GEO and GNE was also conducted. Figure 4 summarizes the antioxidant data for each test in order to compare the antioxidant activity of the free (GEO) and encapsulated essential oils (GNE). There was no discernible difference $p < 0.05$ between the values of the free and encapsulated essential oils in the majority of the tests. This indicates that the antioxidant activity of the essential oil was unaffected by its encapsulation in nanoemulsions. Following GEO encapsulation, it was shown that the assay values of GNE in all tests did not significantly alter, suggesting that GEO remained stable and active with intact antioxidant properties. Notably, it was observed that after encapsulation of GEO, there was a dramatic increase in DPPH scavenging activity values of GNE (Figure 4). Earlier studies have reported that encapsulation techniques improve the bio-efficacy of EOs used as botanical preservatives by enhancing their stability, antimicrobial activity, antimycotoxigenic potential and antioxidant activity. Overall, these investigations conclude that the presence of major along with several minor bioactive phytocomponents in GEO is responsible for the creation of GNE, which is endowed with strong antioxidant properties. The findings are consistent with prior research [32] that found essential oil from oleo-gum resin secreted by *Boswellia serrata* has a great capacity to scavenge free radicals. It was also demonstrated that *B. carterii* essential oil exhibited exceptional capacity to neutralize DPPH radicals (51.68%) [33]. *B. sacra* essential oil was shown to have DPPH- and ABTS-radical scavenging activity, of 57.50% and 48.66%, respectively, in another study [9].

Furthermore, Kasali et al. (2002) [34] reported that compounds such as caryophyllene, limonene, and linalool discovered in our GEO demonstrated significant ferric-reducing and antiradical power activity. As per Khan et al. (2012) [30], the degree of polymerization, concentration, and chemical structure of antioxidants were shown to be associated with their antioxidant activity against DPPH and ABTS. The highest contribution to the antioxidant activity of essential oils may come from oxygenated monoterpenes, most likely from monoterpenoid ketones, as previously shown by Viuda-Martos et al. (2010) [35]. Several scientists have related the antioxidant activity of essential oils to the presence of substances such as verbenone, borneol alcoholic ethers and phenolic compounds, 1,8-cineol, α-pinene, β-pinene, α-thujene, β-thujone, trans-caryophyllene, borneol, and camphor [10].

3.5. Alpha- amylase inhibition assay of GNE

As seen in Figure 4, the α-amylase inhibitory capacity of GNE was ascertained. Figure 5 depicts that GNE demonstrated very effective activity, and showed 70% inhibition at 250 µL volume, whereas synthetic drug acarbose showed 50% inhibition at a dose of 10 µg/mL. Treating diabetes mellitus involves blocking the activity of enzymes like α-amylase, which breaks down sugars and carbohydrates. As a result, there is less gastrointestinal glucose absorption, which reduces blood sugar levels in the body [36]. Further, a comparative study of pure GEO and GNE was also conducted. Notably, it was observed that after encapsulation of GEO, there was no change in α-amylase inhibitor potential of GNE**.** The Lineweaver-Burk (LB) plot was utilized to ascertain the mode of inhibition of GNE. LB plot illustrated that GNE inhibited α-amylase in a competitive manner. It indicated that active components of the GEO and the substrate compete for binding to the α-amylase enzyme active site, thus inhibiting the breakdown of oligosaccharides into disaccharides.

Earlier studies indicate that phytochemicals such as flavonoids can inhibit α-amylase activity, and are primarily responsible for the inhibitory effect of plant extracts [37]. The flavonoids, saponins, and tannins, among other phytochemicals, that are present in the GEO may be responsible for its inhibitory effects. According to earlier research by Najibullah et al. (2021) [38], the presence of active components including limonene, caryophyllene oxide, and linalool in essential oil showed promising inhibitory potential on α-amylase. The essential oils of *Teucrium polium* and *Musca domestica* are rich

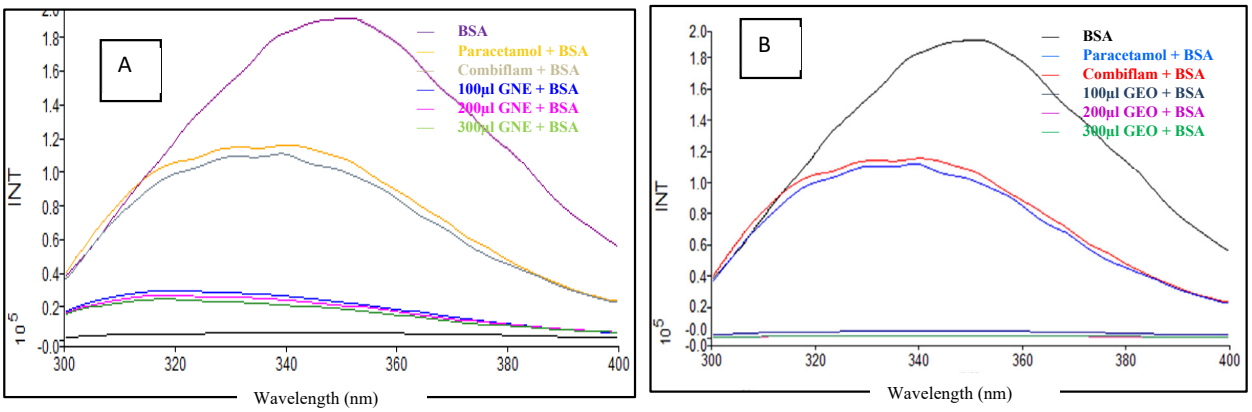

Figure 5. Fluorescence spectroscopy profile (representative) depicting effect of GNE (A) and GEO (B), on BSA protein denaturation at different volumes. INT: intensity

Table 2. Antibacterial activity (in terms of zone of inhibition) of GNE formulation at various volumes on different bacterial strains.

S. NO.	Volume of sample (µL)	Zone of inhibition (ZOI, cm)			
		Pseudomonas aeruginosa, MTCC 424	*Escherichia coli*, MTCC 40	*Staphylococcus aureus*, MTCC 3160	*Bacillus subtilis*, MTCC 121
1	100	0.3 ± 0.02a	0.3 ± 0.01a	NI	NI
2	200	0.4 ± 0.03a	0.5 ± 0.03b	0.2 ± 0.01a	NI
3	300	0.5 ± 0.02b	0.6 ± 0.04b	0.4 ± 0.03b	0.2 ± 0.01a
4	PC	0.8 ± 0.02a	0.8 ± 0.02a	0.3 ± 0.05c	1.1 ± 0.03b

ZOI= zone of inhibition, PC: positive control, NI = nil inhibition. a, b, c letters shows significant difference of data values at P <0.05 with in column. Values are mean ± SD (n=3).

sources of monomers that may have the potential to act as anti-diabetics, according to a study by Riyaphan et al. (2021) [39]. According to our research, GEO's bioactive chemicals caryophyllene, limonene, and linalool can be employed as anti-diabetic medications, which need further validation using *in vivo* models.

3.6. Anti-inflammatory activity (protein denaturation) of GNE formulation

In the current work, the degree of protein denaturation inhibition mediated by GNE was measured using the fluorescence method [19-21]. Therefore, the water-based protein BSA (bovine serum albumin) was used to investigate the anti-inflammatory effects of GNE. Figure 5 shows the usual fluorescence spectra of BSA, BSA + GNE, BSA + combiflam, and BSA + paracetamol. The addition of GNE (100–300 µL) to BSA resulted in a considerable decrease in fluorescence intensity, suggesting a dose-dependent suppression of protein denaturation. This suggested that GNE considerably inhibited protein denaturation. It was shown that the maximum reduction in protein denaturation occurred with 300 µL of GNE. The addition of GNE, for instance, quenched the fluorescent signal, causing its intensity to drop from 1.8×10^5 intensity units to 0.2×10^5 intensity units. Notably, fluorescence quenching was more noticeable with GNE when findings were compared to synthetic medications (paracetamol and combiflam) employed as reference substances. Synthetic medicines reduced the fluorescence signal up to 1.2×10^5 intensity units, but GNE was able to quench the fluorescent signal almost completely. These results offer compelling evidence for the anti-inflammatory qualities of GNE.

Furthermore, a comparison between pure GEO and GNE was carried out. The protein denaturation activity values of GNE did not significantly change following GEO encapsulation, suggesting that GEO remained active with intact protein denaturation activity following encapsulation. The activity of essential oils is attributed to the combined anti-inflammatory qualities of compounds such as β-caryophyllene (19.62%), *α*-pinene (0.082%), and linalool (5.7%). The anti-inflammatory properties of linalool have already been demonstrated [7]. Caryophyllene and linalool were the primary constituents of *Boswellia serrata* essential oil. This supports the findings presented by Kohoude et al. (2017) [40], who stated that the anti-inflammatory impact is caused by these bioactive molecules. More research into the anti-inflammatory properties of GNE is warranted using *in vivo* models.

3.7. Antibacterial activity of GNE formulation

GNE depicted dose-dependent antibacterial activity (Table 2). At 300 µL, GNE showed a 0.6 cm inhibitory zone and strong antibacterial action towards *Escherichia coli* (MTCC 40, Gram-negative). GNE showed a moderate level of efficacy against pathogenic bacteria such as *Pseudomonas aeruginosa* (MTCC 424, Gram-negative) and *Staphylococcus aureus* (MTCC 3160, Gram-positive), with an inhibition zone between 0.4 and 0.5 cm at a volume of 300 µL. Weak antibacterial activity against *Bacillus subtilis* (MTCC 121, Gram-positive) was observed

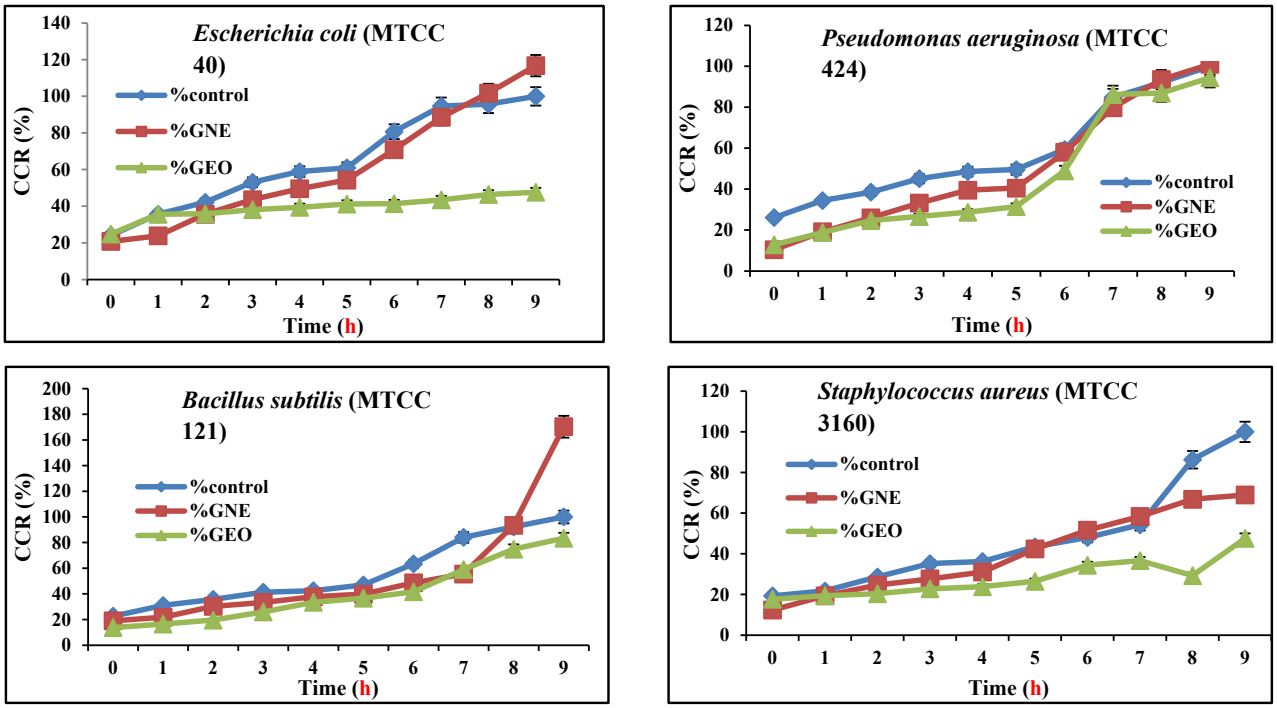

Figure 6. Effect of GNE formulation showing the percentage cytoplasmic content release (CCR, %) on different bacterial strains at different time intervals. Values are mean (n **= 3) ± SD**.

at 300 µL, with an inhibition zone of 0.2 cm. The difference in GNE's antibacterial activity against tested pathogens might be due to the existence of multiple targets or a single target. The antimicrobial activity of GEO may be due to the chemical makeup of GNE and its abundance of major and minor bioactive components that affect the suppression of hydrolysis-related enzymes (proteases) or diminished PARs (microbial adhesions and cell wall envelope proteins) [7].

Furthermore, it has been proposed that the antibacterial qualities of the gum resin *Boswellia serrata's* essential oil may be due to the presence of monoterpenes and oxygenated monoterpenes [4,6]. Previous studies have shown that the efficiency of antimicrobial agents varies and is dependent on several factors, such as their chemical composition [9]. According to earlier research, limonene and linalool prevent several Gram-positive bacterial strains from growing [10]. According to earlier research, antimicrobial activity was sometimes linked to the synergistic effects of major and minor chemical components rather than the high concentration of a single main chemical molecule [41]. A striking finding from our investigation was that GNE showed substantial antimicrobial activity toward Gram-negative bacteria. This is interesting because previous research suggested that Gram-negative bacteria are more resistant than Gram-positive bacteria because they have a thicker cell wall.

3.8. Membrane integrity assay of GNE

The membrane integrity assay of GNE is depicted in Figure 6. GNE showed antibacterial efficacy depending on the pathogen tested. Additionally, all of the bacterial cells treated with GNE showed a linear rise in CCR (%). After 12 hours of incubation, MTCC 121 and MTCC 3160 cells treated with GNE discharged 100% of their cytoplasmic content. In contrast, after 12 hours of incubation, MTCC 424 and MTCC 40 showed 68% and 93% CCR, respectively. GNE was shown to have almost the same CCR% as the reference control Triton-X-100. The outcomes of zone of inhibition experiments used to evaluate antibacterial activity can support these GNE-based conclusions. The bacterial cell membrane is responsible for several important functions, including peptidoglycan cross-linking, lipid

production, transport, and osmoregulation. The integrity of the bacterial membrane is essential for bacterial survival, and its disruption can cause cell death either directly or indirectly, according to Daima et al. (2014) [42]. According to Sugumar et al. (2014) [43], neem-based nanoemulsions may cause rod-shaped bacteria to be disrupted in an indiscriminate manner, which might change and cause cellular components to seep out.

3.9. Cytotoxicity assay of GNE formulation

Figure 7 illustrates how cell viability decreased significantly in a concentration-dependent manner when compared to the control. As seen in Figure 8, compared to untreated control cells, cell viability was markedly decreased with each of the three nanoemulsion doses. The GNE 2 µL and 5 µL doses were more effective in lowering the viability of the cells. Following treatment with 1 µL, 2 µL, and 5 µL GNE, the percentage of viable cells was 90%, 43%, and 20%, respectively. It's interesting to note that paclitaxel was less successful than GNE.

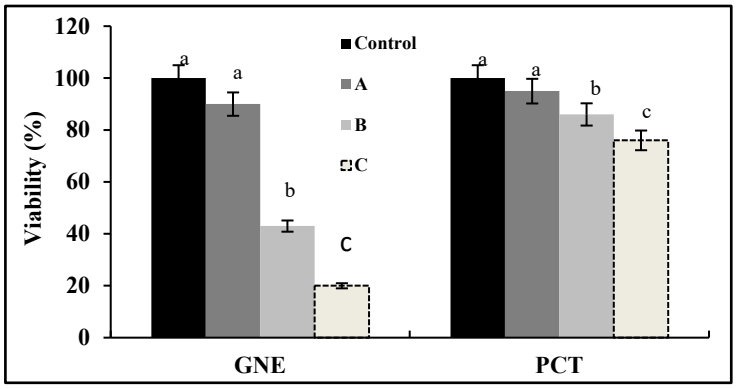

Figure 7. *Effect of GNE formulation on cell viability of HeLa cells. A, B and C represents 1 µL, 2 µL and 5 µL volume for nanoemulsion bars, respectively, and 2 nM, 5 nM and 10 nM for paclitaxel bar, respectively. PCT: paclitaxel. Values are mean (n* **= 3) ± SD. The means followed by same letter at top of the bar are not significantly different at P < 0.05.**

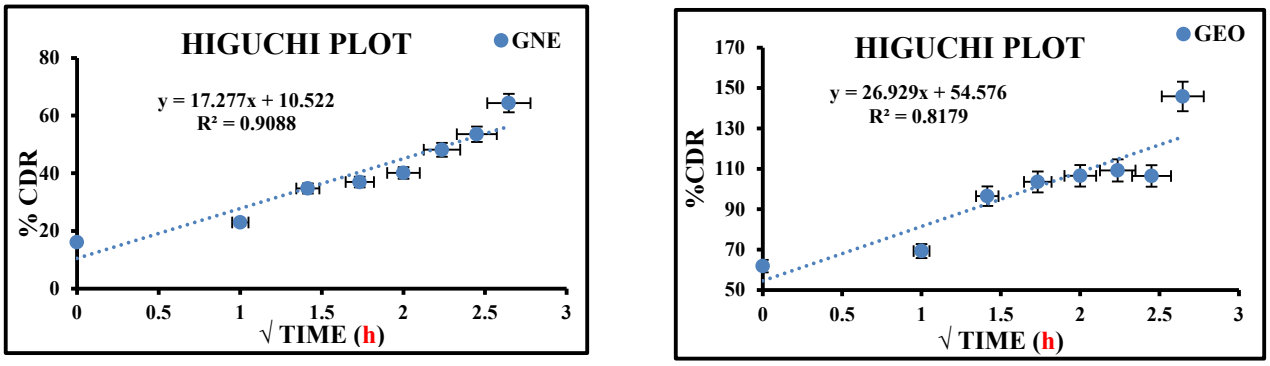

Figure 8. Best-fit drug release profile (Higuchi plot) of GNE and GEO.

There were 95%, 86%, and 76% viable cells after 24 hours of paclitaxel treatment at concentrations of 2 nM, 5 nM, and 10 nM, respectively. This suggests that the GNE has a potent cytotoxic impact.

The findings were corroborated by Eid et al. (2022) [44], who reported that the nanoemulgel exhibited cytotoxic activity when applied to human cervical epithelioid carcinoma cells (HeLa) and hepatocellular carcinoma cells (Hep3B), with IC_{50} values of 28.84, 28.18, and 24.54 µg/mL, respectively, indicating the anticancer effects of the material.

3.10. Drug content, *in vitro* drug release study, and drug release profile of GNE formulation

To get a better understanding of the drug release mechanism, four kinetic models were evaluated: zero-order (%CDR vs. Time), first-order (%Log CDR vs. Time), Korsmeyer-Peppas type (%Log CDR vs. Time), and the Higuchi model (%CDR vs. Square root of Time). Each model describes a specific release mechanism based on different kinetic parameters. The process by which GEO is released from GNE was ascertained using these models. The mechanism by which a drug exits a drug product and subsequently becomes available for pharmacological effect is shown by these models. The best model for explaining the GEO's diffusion pattern was indicated by high correlation coefficient (R^2) values. R^2 values were as follows: 0.90 for the Higuchi model, 0.84 for the Korsmeyer-Peppas type, 0.66 for zero-order, and 0.50 for first-order.

Higuchi was the best-fitting kinetic model, with a higher R^2 value than other kinetic models, based on drug release data (Figure 8). It was hypothesized that several processes were influencing the drug release since a tight association was also observed with Korsmeyer plots, with an R^2 value of 0.84, suggesting an anomalous diffusion mechanism or diffusion combined with erosion. Similar findings were also reported by Merchant et al. (2006) [45] in their investigation of cefpodoxime release assessment in vitro using hydroxypropyl methylcellulose. Our findings are in line with those of Mehrandish and Mirzaeei (2022) [46], who mentioned itraconazole-based nanoemulsions and demonstrated the Higuchi model with an observed R^2 value of 0.9145.

4. Conclusion

In summary, GNE exhibited spherical morphology. Since there was no evidence of separation of phases, cracking, or flocculation in cold circumstances, GNE stayed stable even after 50 days in storage. Strong anti-inflammatory, antibacterial, antioxidant, and antidiabetic effects were also demonstrated by GNE. GNE has also shown potent anticancer activity against cervical cancer cell lines; hence, it can be used as an anticancer agent in combination with anticancer drugs. Because GNE has antioxidant and antibacterial properties, it can be used

to keep food fresher longer by preventing oxidation and microbiological contamination. A theory was formulated based on these results, suggesting that in the future, *Boswellia serrata* essential oil-based nanoemulsions will be a cost-effective approach with significant potential in the food, pharmaceutical, and cosmetic industries. Further studies using *in vivo* models are needed to verify the possibility of using GNE as an anti-diabetic, anti-inflammatory, or food preservation agent.

Acknowledgements

The authors wish to thank Dept of Science and Technology, Govt. of India, DST/SEED/SCSP/STI/2019/253 for funding purposes.

Competing Interests (Include Appropriate Disclosures):

The authors declare that they have no competing interests.

References

1. Mohamed AA, Alotaibi BM. Essential Oils of Some Medicinal Plants and Their Biological Activities: a Mini Review. J Umm Al-Qura Univ Appl Sci. 2023;9(1):40-49. https://doi.org/10.1007/s43994-022-00018-1
2. Kodoh J, Mojiol AR, Lintangah W, Gisiu F, Maid M, Liew KC. Traditional Knowledge of the Uses of Medicinal Plants Among the Ethnic Communities in Kudat, Sabah, Malaysia. Int J Agric For Planta. 2017;5:79-85.
3. Bogavac MA, Perić TM, Mišković J, Karaman M. Antimicrobial and Toxic Effects of Boswellia serrata Roxb. and Mentha piperita Linn. Essential Oils on Vaginal Inhabitants. Medicines (Basel). 2022;9(12):62. https://doi.org/10.3390/medicines9120062
4. Sultana A, Rahman KU, Padmaja AR, Rahman SU. Boswellia serrata Roxb. a Traditional Herb with Versatile Pharmacological Activity: A Review. Int J Pharm Sci Res. 2013;4(6):2106-2119.
5. Alraddadi BG, Shin HJ. Biochemical Properties and Cosmetic Uses of Commiphora myrrha and Boswellia serrata. Cosmetics. 2022;9(6):119. https://doi.org/10.3390/cosmetics9060119
6. Hussain H, Al-Harrasi A, Al-Rawahi A, Hussain J. Chemistry and Biology of Essential Oils of Genus Boswellia. Evid Based Complement Alternat Med. 2013;2013:140509. https://doi.org/10.1155/2013/140509
7. Siddiqui MZ. Boswellia serrata, a Potential Antiinflammatory Agent: an Overview. Indian J Pharm Sci. 2011;73(3):255-261.
8. Ni X, Suhail MM, Yang Q, Cao A, Fung KM, Postier RG, et al. Frankincense Essential Oil Prepared from Hydrodistillation of Boswellia sacra Gum Resins Induces Human Pancreatic Cancer Cell Death in Cultures and in a Xenograft Murine Model. BMC Complement Altern Med. 2012;12(1):253. https://doi.org/10.1186/1472-6882-12-253
9. Al-Saidi S, Rameshkumar KB, Hisham A, Sivakumar N, Al-Kindy S. Composition and Antibacterial Activity of the Essential Oils of Four Commercial Grades of Omani Luban, the Oleo-Gum Resin of Boswellia sacra Flueck. Chem Biodivers. 2012;9(3):615-624. https://doi.org/10.1002/cbdv.201100189
10. Camarda L, Dayton T, Di Stefano V, Pitonzo R, Schillaci D. Chemical Composition and Antimicrobial Activity of Some Oleogum Resin Essential Oils from Boswellia spp. (Burseraceae). Ann Chim. 2007;97(9):837-844. https://doi.org/10.1002/adic.200790068
11. Turek C, Stintzing FC. Stability of Essential Oils: A Review. Compr Rev Food Sci Food Saf. 2013;12(1):40-53. https://doi.org/10.1111/1541-4337.12006
12. Agostinho LC, Attademo M, Oliveira MPA, Rocha-Filho PA. Development of Nanoemulsion with Vegetal Oils Enhanced by Melaleuca and Lavender Essential Oils. Int J Nanosci Nanotechnol. 2022;18(4):233-240.
13. Zakarya Nezhad N, Moradi H, Biparva P, Memariani Z. Comparative Study on Preparation, Characterization and Antioxidant Activity of Encapsulated Viola odorata L. Extract Based on Gum Arabic-Gelatin and Lepidium perfoliatum L. Seed Gum Nanoemulsions. Int J Nanosci Nanotechnol. 2024;20(1):47-61.
14. Donsi F. Applications of Nanoemulsions in Foods. In: Jafari SM, McClements DJ, editors. Nanoemulsions: Formulation, Applications, and Characterization. Cambridge, MA: Academic Press; 2018. p. 349-377. https://doi.org/10.1016/B978-0-12-811838-2.00011-4
15. Chang Y, McLandsborough L, McClements DJ. Fabrication, Stability and Efficacy of Dual-Component Antimicrobial Nanoemulsions: Essential Oil (Thyme Oil) and Cationic Surfactant (Lauric Arginate). Food Chem. 2015;172:298-304. https://doi.org/10.1016/j.foodchem.2014.09.081
16. Yan H, Bao C, Chen X, Yu C, Kong D, Shi J, et al. Preparation of Biodiesel Oil-in-Water Nanoemulsions by Mixed Surfactants for Bifenthrin Formulation. RSC Adv. 2019;9(21):11649-11658. https://doi.org/10.1039/C9RA00591A
17. Jaiswal M, Dudhe R, Sharma PK. Nanoemulsion: an Advanced Mode of Drug Delivery System. 3 Biotech. 2015;5(2):123-127. https://doi.org/10.1007/s13205-014-0214-0
18. Nagajyothi M, Pramod K, Bijin EN, Baby JN, Valsalakumari J. Nanoemulsified System of a Poorly Water Soluble Drug. Res J Pharm Dos Forms Technol. 2015;7(3):169-174. https://doi.org/10.5958/0975-4377.2015.00025.7
19. Salvia-Trujillo L, Rojas-Graü MA, Soliva-Fortuny R, Martín-Belloso O. Effect of Processing Parameters on Physicochemical Characteristics of Microfluidized Lemongrass Essential Oil-Alginate Nanoemulsions. Food Hydrocoll. 2013;30(1):401-407. https://doi.org/10.1016/j.foodhyd.2012.07.004
20. Sharma AD, Kaur I, Amrita, Devi R. Phytochemical profile using GC-FID and diverse in vitro biological activities of essential oil extracted from Boswellia serrata. Arab J Med Aromat Plants. 2023;9(1):1-37.
21. Chauhan A, Jain P, Kaur I, Chhabra R, Sharma AD. Preparation, characterization and in vitro bioassays of nanoemulsions from palmarosa (Cymbopogon martinii) essential oil. J Dispers Sci Technol. 2024;46(2):1-18. https://doi.org/10.1080/01932691.2024.2317839
22. Bernardi DS, Pereira TA, Maciel NR, Bortoloto J, Viera GS, Oliveira GC, et al. Formation and Stability of Oil-in-Water Nanoemulsions Containing Rice Bran Oil: In Vitro and In Vivo Assessments. J Nanobiotechnology. 2011;9(1):44. https://doi.org/10.1186/1477-3155-9-44
23. Sutradhar KB, Amin ML. Nanoemulsions: Increasing Possibilities in Drug Delivery. Eur J Nanomed. 2013;5(2):97-110. https://doi.org/10.1515/ejnm-2013-0001
24. Moradi S, Barati A. Essential Oils Nanoemulsions: Preparation, Characterization and Study of Antibacterial Activity Against Escherichia coli. Int J Nanosci Nanotechnol. 2019;15(3):199-210.
25. Baboota S, Shakeel F, Ahuja A, Ali J, Shafiq S. Design Development and Evaluation of Novel Nanoemulsion Formulations for Transdermal Potential of Celecoxib. Acta Pharm. 2007;57(3):315-332. https://doi.org/10.2478/v10007-007-0025-5
26. Heydari R, Rashidipour M, Naleini N. Determination of Efavirenz in Plasma by Dispersive Liquid-Liquid Microextraction Coupled to High-performance Liquid Chromatography. Curr Anal Chem. 2014;10(2):280-287. https://doi.org/10.2174/1573411011309990003
27. Laxmi M, Bhardwaj A, Mehta S, Mehta A. Development and Characterization of Nanoemulsion as Carrier for the Enhancement of Bioavailability of Artemether. Artif Cells Nanomed Biotechnol. 2015;43(5):334-344. https://doi.org/10.3109/21691401.2014.887018

28. Farooq U, Rasul A, Zafarullah M, Abbas G, Rasool M, Ali F, et al. Nanoemulsions as Novel Nanocarriers for Drug Delivery Across the Skin: In-Vitro, In-Vivo Evaluation of Miconazole Nanoemulsions for Treatment of Candidiasis albicans. Des Monomers Polym. 2021;24(1):240-258. https://doi.org/10.1080/15685551.2021.1965724
29. Boni M, Nastasa V, Andrei IR, Staicu A, Pascu ML. Enhanced Fluorescence Emitted by Microdroplets Containing Organic Dye Emulsions. Biomicrofluidics. 2015;9(1):014126. https://doi.org/10.1063/1.4913648
30. Khan RA, Khan MR, Sahreen S, Ahmed M. Assessment of Flavonoid Contents and In Vitro Antioxidant Activity of Launaea procumbens. Chem Cent J. 2012;6(1):43. https://doi.org/10.1186/1752-153X-6-43
31. Monago-Maraña O, Cabrera-Bañegil M, Rodas NL, Muñoz de la Peña A, Durán-Merás I. First-Order Discrimination of Methanolic Extracts from Plums According to Harvesting Date Using Fluorescence Spectra. Quantification of Polyphenols. Microchem J. 2021;169:106533. https://doi.org/10.1016/j.microc.2021.106533
32. Gupta M, Rout P, Misra L, Gupta P, Singh N, Darokar M, et al. Chemical Composition and Bioactivity of Boswellia serrata Essential Oil in Relation to Geographical Variation. Plant Biosyst. 2016;151(4):623-629. https://doi.org/10.1080/11263504.2016.1187681
33. Prakash B, Mishra PK, Kedia A, Dubey NK. Antifungal, Antiaflatoxin and Antioxidant Potential of Chemically Characterized Boswellia carterii Birdw Essential Oil and Its In Vivo Practical Applicability in Preservation of Piper nigrum L. Fruits. LWT Food Sci Technol. 2014;56(2):240-247. https://doi.org/10.1016/j.lwt.2013.12.023
34. Kasali AA, Adio AM, Oyedeji AO, Eshilokun AO, Adefenwa M. Volatile Constituents of Boswellia serrata Roxb. (Burseraceae) Bark. Flavour Fragr J. 2002;17(6):462-464. https://doi.org/10.1002/ffj.1124
35. Viuda-Martos M, Ruiz Navajas Y, Sánchez Zapata E, Fernández-López J, Pérez-Álvarez JA. Antioxidant Activity of Essential Oils of Five Spice Plants Widely Used in a Mediterranean Diet. Flavour Fragr J. 2010;25(1):13-19. https://doi.org/10.1002/ffj.1951
36. Mccue P, Kwon YI, Shetty K. Anti-amylase, Anti-glucosidase and Anti-angiotensin I-Converting Enzyme Potential of Selected Foods. J Food Biochem. 2005;29(3):278-294. https://doi.org/10.1111/j.1745-4514.2005.00020.x
37. Kazeem MI, Adamson JO, Ogunwande IA. Modes of Inhibition of α-Amylase and α-Glucosidase by Aqueous Extract of Morinda lucida Benth Leaf. Biomed Res Int. 2013;2013:527570. https://doi.org/10.1155/2013/527570
38. Najibullah SNM, Ahamad J, Aldahish AA, Sultana S, Sultana S. Chemical Characterization and α-Glucosidase Inhibitory Activity of Essential Oil of Lavandula angustifolia Flowers. J Essent Oil Bear Plants. 2021;24(3):431-438. https://doi.org/10.1080/0972060X.2021.1942233
39. Riyaphan J, Pham D, Leong MK, Weng CF. In Silico Approaches to Identify Polyphenol Compounds as α-Glucosidase and α-Amylase Inhibitors Against Type-II Diabetes. Biomolecules. 2021;11(12):1877. https://doi.org/10.3390/biom11121877
40. Kohoude MJ, Gbaguidi F, Agbani P, Ayedoun MA, Cazaux S, Bouajila J. Chemical Composition and Biological Activities of Extracts and Essential Oil of Boswellia dalzielii Leaves. Pharm Biol. 2017;55(1):33-42. https://doi.org/10.1080/13880209.2016.1226356
41. Jerobin J, Makwana P, Kumar RS, Sundaramoorthy R, Mukherjee A, Chandrasekaran N. Antibacterial Activity of Neem Nanoemulsion and Its Toxicity Assessment on Human Lymphocytes In Vitro. Int J Nanomedicine. 2015;10(Suppl 1):77-86. https://doi.org/10.2147/IJN.S79983
42. Daima HK, Selvakannan PR, Kandjani AE, Shukla R, Bhargava SK, Bansal V. Synergistic Influence of Polyoxometalate Surface Corona Towards Enhancing the Antibacterial Performance of Tyrosine-Capped Ag Nanoparticles. Nanoscale. 2014;6(2):758-765. https://doi.org/10.1039/C3NR03806H
43. Sugumar S, Ghosh V, Nirmala MJ, Mukherjee A, Chandrasekaran N. Ultrasonic Emulsification of Eucalyptus Oil Nanoemulsion: Antibacterial Activity Against Staphylococcus aureus and Wound Healing Activity in Wistar Rats. Ultrason Sonochem. 2014;21(3):1044-1049. https://doi.org/10.1016/j.ultsonch.2013.10.021
44. Eid AM, Jaradat N, Issa L, Abu-Hasan A, Salah N, Dalal M, et al. Evaluation of Anticancer, Antimicrobial, and Antioxidant Activities of Rosemary (Rosmarinus officinalis) Essential Oil and Its Nanoemulgel. Eur J Integr Med. 2022;55:102175. https://doi.org/10.1016/j.eujim.2022.102175
45. Merchant HA, Shoaib HM, Tazeen J, Yousuf RI. Once-daily tablet formulation and in vitro release evaluation of cefpodoxime using hydroxypropyl methylcellulose: a technical note. AAPS PharmSciTech. 2006;7(1):E178-E183. https://doi.org/10.1208/pt070378
46. Mehrandish S, Mirzaeei S. Design of Novel Nanoemulsion Formulations for Topical Ocular Delivery of Itraconazole: Development, Characterization and In Vitro Bioassay. Adv Pharm Bull. 2022;12(1):93-101. https://doi.org/10.34172/apb.2022.009